Phosphoinositide 3-kinase γ/δ inhibition limits infarct size after myocardial ischemia/reperfusion injury

John Doukas*†, Wolfgang Wrasidlo*‡, Glenn Noronha*, Elena Dneprovskaia*, Richard Fine§, Sara Weis¶, John Hood*, Anthony DeMaria‖, Richard Soll*, and David Cheresh¶

*TargeGen, Inc., 9380 Judicial Drive, San Diego, CA 92121; §BioPredict, Inc., 660 Kinderkamack Road, Oradell, NJ 07649; ¶University of California at San Diego, Moores Cancer Center, 3855 Health Sciences Drive, La Jolla, CA 92093; and ‖University of California at San Diego Medical Center, Division of Cardiology, 200 West Arbor Drive, San Diego, CA 92103

Edited by Peter K. Vogt, The Scripps Research Institute, La Jolla, CA, and approved October 20, 2006 (received for review August 11, 2006)

Although phosphoinositide 3-kinases (PI3Ks) play beneficial pro-cell survival roles during tissue ischemia, some isoforms (γ and δ) paradoxically contribute to the inflammation that damages these same tissues upon reperfusion. We therefore considered the possibility that selectively inhibiting proinflammatory PI3K isoforms during the reperfusion phase could ultimately limit overall tissue damage seen in ischemia/reperfusion injuries such as myocardial infarction. Panreactive and isoform-restricted PI3K inhibitors were identified by screening a novel chemical family; molecular modeling studies attributed isoform specificity based on rotational freedom of substituent groups. One compound (TG100-115) identified as a selective PI3K γ/δ inhibitor potently inhibited edema and inflammation in response to multiple mediators known to participate in myocardial infarction, including vascular endothelial growth factor and platelet-activating factor; by contrast, endothelial cell mitogenesis, a repair process important to tissue survival after ischemic damage, was not disrupted. In rigorous animal MI models, TG100-115 provided potent cardioprotection, reducing infarct development and preserving myocardial function. Importantly, this was achieved when dosing well after myocardial reperfusion (up to 3 h after), the same time period when patients are most accessible for therapeutic intervention. In conclusion, by targeting pathologic events occurring relatively late in myocardial damage, we have identified a potential means of addressing an elusive clinical goal: meaningful cardioprotection in the post-reperfusion time period.

edema | inflammation | myocardial infarct | VEGF

Myocardial infarction (MI) results from a biphasic ischemia/reperfusion (I/R) injury to the heart, initiating with cardiomyocyte apoptosis (1), then proceeding to a second wave of inflammation-based tissue damage (2). Despite considerable effort, therapeutic interventions to disrupt this injury pattern have not translated well from preclinical studies into the clinic. One major limitation has been a focus on antiischemia therapies that require delivery early in MI pathogenesis, a time when the great majority of patients are inaccessible (3). By contrast, although reperfusion injury does unfold in the appropriate interventional setting, inflammation's multifactorial nature complicates attempts to limit its impact. For example, proinflammatory mediators generated during I/R injury include VEGF (4), platelet-activating factor (PAF) (5), multiple cytokines and eicosanoids (6–8), histamine (9), thrombin (10), and complement factors (11). Although this diversity makes blockade at the receptor level unfeasible, inhibition at the subreceptor level would be reasonable were a common signaling element identifiable.

Phosphoinositide 3-kinase (PI3K) could represent this gatekeeper, lying downstream of both receptor tyrosine kinases and G protein-coupled receptors (GPCR), two receptor classes encompassing the ligands listed above. The γ and δ isoforms in particular would appear promising targets, because genetic deletion studies establish their roles in edema and inflammatory responses (12–17). By contrast, PI3Kα and -β, two broadly expressed isoforms, apparently play more fundamental biologic roles, because genetic deletion of either is lethal (18).

Along with possible pitfalls from disrupting developmental events, anti-PI3K therapies are also complicated by the potential for proapoptotic activity. Considerable evidence supports a prosurvival role for PI3K (and its downstream target, Akt) during ischemia (19) and, although the exact isoform(s) involved remain unclear, in general PI3K pathways are considered beneficial events that should not be disrupted during I/R injuries (20, 21). Additionally, although commonly used PI3K inhibitors reduce inflammatory events in animal models (22), they have failed to reduce infarct size when delivered after reperfusion (23). Finally, transgenic mice overexpressing a kinase-inactive PI3Kγ in their cardiomyocytes develop infarcts of equivalent size as do wild-type animals after I/R injury (24). On the whole, then, it seems at best equivocal whether inhibition of PI3K signaling would prove beneficial, detrimental, or inconsequential to infarct development.

As a step toward resolving this question, we now report our experience using a previously undescribed PI3Kγ/δ inhibitor to interrupt the reperfusion phase of I/R injury. This small molecule (TG100-115) was confirmed as a potent inhibitor of edema and inflammation induced by both receptor tyrosine kinase and GPCR ligands, but which at the same time spared tissue repair processes such as endothelial cell (EC) mitogenesis. In MI models designed to aggressive standards, it both reduced infarct development and improved myocardial function. Most impressively, cardioprotection was seen upon delivery up to several hours after reperfusion, a time when MI patients are available for therapeutic intervention in acute care settings, supporting our hope that this approach to selective PI3K isoform inhibition holds promise for bridging that gap between preclinical efficacy and clinical utility.

Results

Identification of PI3K Isoform-Selective Inhibitors. Screening a novel family of pteridines for activity against class IA (α, β, δ) and IB

Author contributions: J.D., W.W., G.N., E.D., J.H., A.D., R.S., and D.C. designed research; J.D., W.W., G.N., E.D., R.F., and S.W. performed research; J.D., W.W., G.N., E.D., R.F., S.W., J.H., A.D., R.S., and D.C. analyzed data; and J.D., R.S., and D.C. wrote the paper.

Conflict of interest statement: J.D., G.N., E.D., J.H., and R.S. are employees of TargeGen, Inc., and hold stock options in the company. W.W. is a former employee of TargeGen, Inc., and holds stock options in the company. A.D. and D.C. serve on the Scientific Advisory Board of TargeGen, Inc., and hold stock options in the company.

This article is a PNAS direct submission.

Freely available online through the PNAS open access option.

Abbreviations: MI, myocardial infarction; I/R, ischemia/reperfusion; PAF, platelet-activating factor; PI3K, phosphoinositide 3-kinase; GPCR, G protein-coupled receptor; EC, endothelial cell; LV, left ventricle; LAD, left anterior descending coronary artery; AAR, area at risk.

†To whom correspondence should be addressed. E-mail: jdoukas@targegen.com.

‡Present address: University of California at San Diego, Moores Cancer Center, Room 2344, 3855 Health Sciences Drive, #0803, La Jolla, CA 92093-0803.

This article contains supporting information online at www.pnas.org/cgi/content/full/0606956103/DC1.

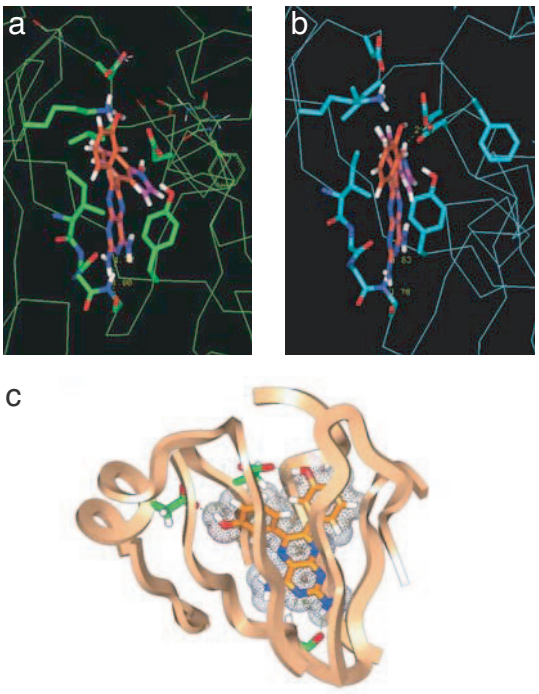

Fig. 1. Models of PI3K isoform-kinase inhibitor interactions. (*a*) Superposition of TG100-115, TG100713, and TG101110 in PI3Kγ showing preferred rotatable angles between ring A and the pteridine core. (*b*) Superposition of the same three compounds in PI3Kα. (*c*) Model structure of human PI3Kγ kinase (ribbon) with TG100-115 located in the catalytic domain.

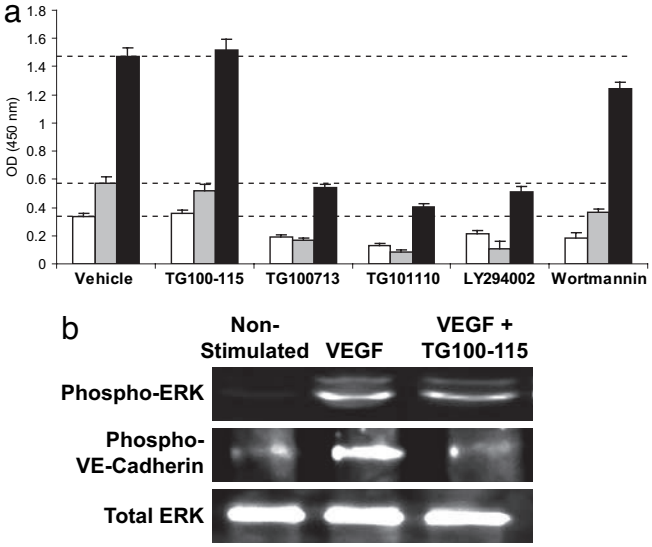

Fig. 2. Inhibition of cell proliferation and signaling. (*a*) EC were cultured in the presence of vehicle (DMSO) or PI3K inhibitors (all at 10 μM); cell proliferation was assessed 24 (open bar), 48 (gray bar), or 72 h (black bar) later. Data are presented as OD at 450 nm (mean $\pm$ SEM, $n = 6$; at all timepoints, vehicle and TG100-115 groups differ from all others but not each other by $P < 0.001$). (*b*) EC were cultured in serum-free medium (nonstimulated), medium with added VEGF, or medium with VEGF plus 10 μM TG100-115. Cell lysates were then processed for Western blot analyses to detect phosphorylated VE-cadherin or ERK1/2, or total ERK2 (as a loading control).

(γ)PI3K isoforms identified panisoform inhibitors (e.g., TG100713), as well as more selective compounds [e.g., TG101110, which spares PI3Kα; supporting information (SI) Table 1]. The most promising compound, TG100-115, inhibited PI3Kγ and -δ (IC_{50} values of 83 and 235 nM, respectively), whereas both PI3Kα and -β were relatively unaffected (IC_{50} values >1 μM). As a gauge of general specificity, TG100-115 was also assayed against a 133 protein kinase panel, none of which were inhibited at IC_{50} values <1 μM (SI Table 2).

Modeling studies indicated that the freedom of conformational rotation permitted by ring substituents governs isoform selectivity (SI Fig. 6). Although TG100-115, TG100713, and TG101110 all allow for substituent ring energy minima at 30–40°, each compound pays differing penalties as angles diverge from this range. TG100-115 exhibits the greatest barrier to rotation (most conformations $\gg$50 kcal) and consequentially is the most isoform selective, TG100713 with the most conformational flexibility (ring A being almost freely rotatable with maxima $\approx$5 kcal; 1 kcal = 4.18 kJ) is the least selective, and TG101110 occupies an intermediate position (several conformations $\leq$10 but some $\gg$50 kcal).

Regarding kinase isoforms, PI3Kγ is most tolerant of ring conformational variations followed by PI3Kδ, supporting a model in which these two kinases are more readily fit by all three compounds; PI3Kα and -β being less tolerant lockout TG100-115 and partially TG101110 (Fig. 1). For TG100-115, modeling supports that two strong hydrogen bonds can form with the PI3Kγ hinge region: the N-3 nitrogen of the pteridine ring serving as an acceptor to the backbone NH of Val-882 and the 2-primary amine group serving as donor to the same residue's backbone carbonyl. Additionally TG100-115's 4-amino group is positioned adjacent to the backbone carbonyl of Glu-880; however, bond formation geometry is poor. These hydrogen bond patterns are similar to those for ATP as seen in the published ATP/PI3Kγ complex 1E8X, supporting a model for TG100-115 binding within the catalytic domain (Fig. 1*c*). Interactions are also formed outside the ATP-binding site, where a pocket accommodates TG100-115's 6′ substituted metaphenol, and Asp-841 (on the kα3 helix at the pocket's rear) forms a hydrogen bond with the OH group.

To place these data in context, two reagents commonly used as PI3K inhibitors were also profiled (SI Table 1). LY294002 was revealed as a relatively weak inhibitor (IC_{50} values against PI3Kδ and -β of 561 and 858 nM, respectively, and no meaningful activity against PI3Kα or -γ); wortmannin, by contrast, displayed activity in the same general potency range as TG100-115 (55–147 nM) but with a panisoform profile.

PI3Kγ/δ Inhibition Selectively Impacts Growth Factor Signaling. PI3K isoforms can differently regulate cellular processes, as with mitogenesis falling under PI3Kα and -β control (18). We therefore compared the compounds profiled in SI Table 1 for their effects on cell proliferation. As expected, panisoform inhibitors (TG100713 and wortmannin) strongly inhibited EC proliferation (Fig. 2*a*). TG101110 and LY294002 displayed similar efficacy, suggesting that either PI3Kα or -β inhibition is sufficient for blocking mitogenesis. TG100-115, by contrast, had no effects on EC proliferation even at relatively high concentrations (up to 10 μM). Additionally, TG100-115 did not block VEGF-induced angiogenesis *in vivo* (using a Matrigel implant model; data not shown). In agreement with these data, this compound was also found to have no influence on VEGF-stimulated ERK phosphorylation (Fig. 2*b*), a signaling event in this growth factor's mitogenic pathway (25). It did, however, interrupt other VEGF signaling pathways, such as those that culminate in VE-cadherin phosphorylation, the culmination of a signaling cascade that underlies VEGF's proedema activity (26). These data indicate that, whereas the non-ERK-related pathway(s) leading to VE-cadherin phosphorylation depend upon intact PI3Kγ and/or -δ activity, those that control cell proliferation are not.

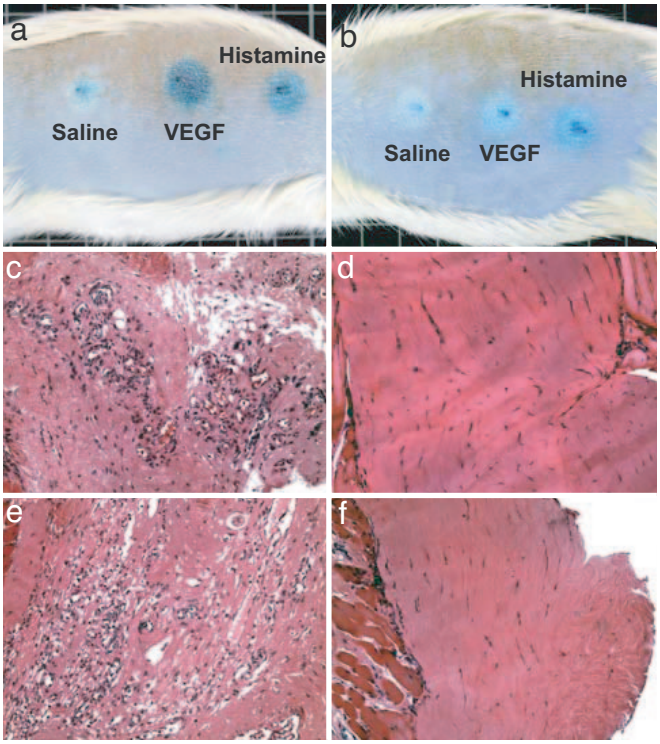

Fig. 3. Inhibition of edema and inflammation. (*a* and *b*) Rats were injected i.v. with Evans blue dye and then intradermally with saline, VEGF, or histamine. Pretreatment with TG100-115 (1 mg/kg) (*b*) reduced edema formation relative to vehicle-treated animals (*a*). (*c–f*) Rat hindpaws were injected with either PAF (*c* and *d*) or dextran (*e* and *f*) and processed 3 h later as H&E-stained paraffin sections. Pretreatment with TG100-115 (*d* and *f*; 5 mg/kg) blocked both the edema and leukocytic infiltrate induced by these two inflammatory mediators relative to animals dosed with vehicle alone (*c* and *e*). Images were taken of paws representing the mean group value for volume as presented in *Results*. (Original magnification ×200.)

PI3Kγ/δ Inhibition Reduces Edema and Inflammation *in Vivo*. Because VE-cadherin phosphorylation triggers a reduction in endothelial barrier function (26), TG100-115's ability to block this cellular event should translate into an antiedema effect. This was directly demonstrated in Miles assay studies, where this compound inhibited VEGF-induced vascular permeability (Fig. 3). TG100-115 also blocked histamine-induced permeability, as predicted based on PI3K's role in GPCR signaling. Varying the time between compound administration and agonist challenge demonstrated that a single i.v. administration reduced edema formation for at least 4 h (data not shown).

The Miles assay models a primarily endothelial-based response that develops rapidly (within minutes). As a comparator, we next used a rodent hindpaw model, where more complex inflammatory reactions develop over several hours. Agonists included PAF, a GPCR ligand that activates both EC and leukocytes, and dextran, a phagocytic stimulus for mast cell and leukocyte activation (27). Histology revealed quite clearly that TG100-115 strongly antagonized both the edema and leukocyte infiltration induced by these two mediators (Fig. 3 *c–f*). Paw volume (a more quantitative measure of edema and inflammation) was reduced by 62% and 78% in response to PAF or dextran, respectively ($n = 8$; $P < 0.001$). Finally, to correlate these *in vivo* responses with the molecular target of interest, we monitored PI3K pathway signaling through Western blot analyses of Akt phosphorylation (a PI3K-mediated event). VEGF injection i.v. in mice induced a rapid Akt phosphorylation readily detectable in lung lysates and, as expected, pretreatment with TG100-115 blocked this response (SI Fig. 7). Blockade was seen with TG100-115 doses as low as 0.5 mg/kg and persisted over a period of several hours.

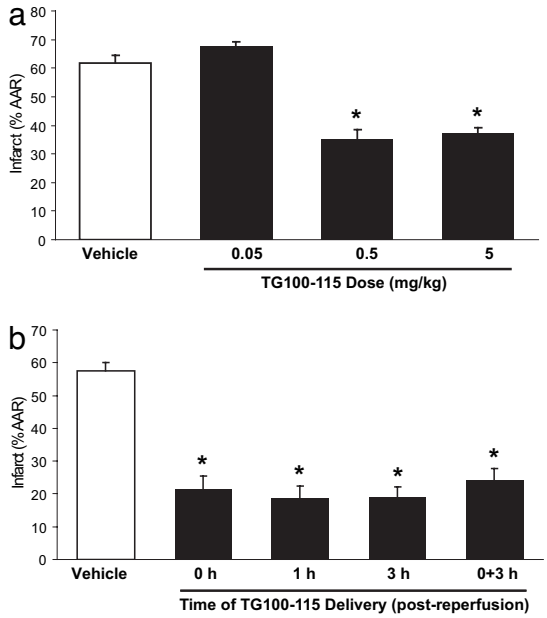

Fig. 4. Reduction of infarct development in a rodent MI model. (*a*) Rats were subjected to 60 min of LAD occlusion followed by vehicle or TG100-115 delivery (at the indicated dose) 60 min after reperfusion. Both ischemic area [area at risk (AAR)] and infarct area were then determined 24 h after study initiation. Data are shown as infarct area as a percentage of the AAR (means ± SEM, $n = 6$; *, 0.5 and 5 mg/kg TG100-115 dose groups differ from vehicle control by $P < 0.05$ but not from one another). (*b*) Animals were treated as in *a*, except that a single TG100-115 dose (0.1 mg/kg) was delivered at 0-3 h after reperfusion; in one group, animals were dosed at both 0 and 3 h. Data shown are as in *a* ($n = 5–9$; *, all TG100-115 groups differ from vehicle control by $P < 0.001$ but not from one another).

PI3Kγ/δ Inhibition Limits Infarct Development and Improves Myocardial Functioning in Rodents. We previously documented in rodents the vascular changes, such as edema and neutrophil activation, which contribute to infarct development (26). Given the antiinflammatory actions of our PI3Kγ/δ inhibitor, therefore, we tested this compound for possible cardioprotective activities. In a rodent model of MI, TG100-115 delivered as a single i.v. bolus 60 min after reperfusion routinely reduced infarct size by ≥40%, with maximal efficacy reached by a dose of 0.5 mg/kg (Fig. 4*a*). [This model initiates with a 60-min coronary artery occlusion followed by complete reperfusion and then infarct measurement at 24 h; in control animals, the ischemic zone typically covers 30–45% of the total left ventricle (LV) with 55–70% infarction of this area. Pilot studies revealed that longer ischemic periods do not produce larger infarcts and that infarcts do not reach a fixed size until ≈6 h after reperfusion.] Immunohistochemistry as well as EM revealed similar patterns of monocyte and neutrophil infiltration in hearts from TG100-115 vs. vehicle-treated animals (data not shown). Although it was obvious that infarcts were smaller in TG100-115 animals, inflammatory infiltrates were present to an equivalent degree in infarcted myocardium from both treatment groups. Inflammation was not detectable, by contrast, in viable tissue (i.e., myocardium not showing morphologic signs of cardiomyocyte or vascular damage). These observations are consistent, therefore, with an action by TG100-115 to reduce the overall area in which inflammation occurs and thus the final extent of infarction.

To better define the available therapeutic window for this

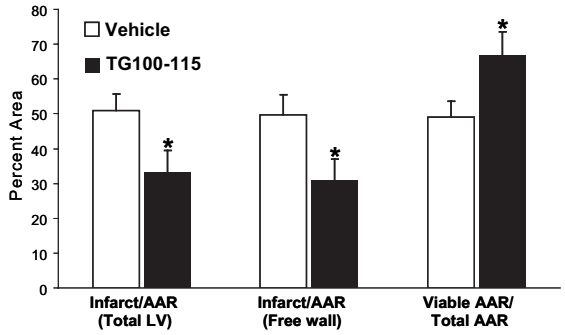

Fig. 5. Reduction of infarct development in a porcine MI model. Pigs were subjected to 90 min of LAD occlusion followed by vehicle or TG100-115 (0.5 mg/kg) delivery 30 min after reperfusion. At 24 h after study initiation, total ischemic area (AAR), viable AAR, and infarcted AAR were determined, for the entire LV as well as the free wall alone. Data are shown as infarct as a percentage of AAR or viable AAR as a percentage of total AAR (means ± SEM, $n = 12–13$; *, vehicle and TG100-115 groups differ for all measures by $P \leq 0.05$).

cardioprotective effect, TG100-115 was administered at various times during the reperfusion period (Fig. 4*b*). Delivery (as a single bolus) between 0 and 3 h after reperfusion produced statistically significant but equivalent reductions in infarct development (in this case 58–67% reductions vs. vehicle-treated controls). Repeat dosing at both 0 and 3 h also provided equivalent efficacy, suggesting that a single administration is sufficient for maximal efficacy. Finally, to confirm the functional benefit of infarct reduction, myocardial contractility was assessed by echocardiography 4 weeks after infarct induction. The percent LV long axis fractional shortening observed in animals that had received vehicle placebo was 27.2 ± 1.9 (mean ± SEM), whereas animals dosed with TG100-115 as a single 0.5 mg/kg bolus 1 h after reperfusion had a 24% improvement in this measure (33.6 ± 2.0, $n = 12–13$; $P = 0.03$). These data therefore confirm a long-lasting functional benefit to PI3Kγ/δ inhibition during myocardial reperfusion injury.

PI3Kγ/δ Inhibition Limits Infarct Development in a Porcine MI Model. In a final series of studies, MIs were modeled in the pig, because this species better approximates human coronary anatomy and responses to myocardial I/R injury. With aggressive model parameters of a 90-min ischemic period, therapeutic dosing 30 min after reperfusion, and infarct measurement at 24 h, we typically observed ischemic zones representing 20–30% of the total LV and 20–30% infarction of this area in control animals. In initial dose-ranging studies, generally equivalent responses were observed using TG100-115 doses of 0.5–10 mg/kg (data not shown), and we therefore elected to conduct a statistically powered test at the lowest dose. Animals dosed with TG100-115 as a single 0.5 mg/kg i.v. bolus 30 min after reperfusion developed smaller infarcts vs. vehicle-treated controls (Fig. 5). Measuring infarct area as percent of total LV ischemic area, infarct size was reduced by 35% ($P = 0.04$). Viable tissue within the ischemic zone was increased by 37% ($P = 0.04$), directly demonstrating the cardioprotective effect of PI3Kγ/δ inhibition. Finally, taking advantage of the larger porcine heart to make more detailed measurements, infarct areas within the LV free wall only (as opposed to the free plus attached wall measurements reported up to this point) were also determined, reasoning that free wall infarcts are of greatest relevance to overall myocardial function. As anticipated, TG100-115 reduced free wall infarct size by 38% vs. vehicle-treated controls ($P = 0.05$).

Discussion

The data presented support our hypothesis that broadly blocking proinflammatory processes can limit I/R injury even well after the initiation of ischemic damage. To achieve this efficacy, we used a previously undescribed kinase inhibitor (TG100-115) selected for three specific properties. First, this compound inhibited PI3Kγ and to a lesser degree PI3Kδ with excellent specificity. Second, it blocked cell signaling events selectively rather than globally. Third, it antagonized both endothelium and leukocyte-associated aspects of inflammation induced by multiple and diverse mediators. As final proof of these properties' value, TG100-115 proved cardioprotective when delivered well into the reperfusion period in both rodent and porcine models of acute MI.

Molecular modeling studies provided a basis for understanding PI3K isoform specificity based on the freedom of conformational rotation permitted by ring substituents, with rotational restrictions resulting in increased specificity. By inhibiting PI3Kγ and -δ while sparing α and β isoforms (as well as a wide range of protein kinases), selective inhibition of inflammation-associated aspects of VEGF signaling was achieved. Of direct relevance to cardioprotection, PI3Kγ/δ inhibition blocked VEGF signaling events that trigger edema (VE cadherin phosphorylation) while sparing those that control mitogenesis (ERK phosphorylation). VEGF plays both positive (proangiogenic) and negative (proedema) roles in I/R injuries, with PI3K regulating both activities (13, 28), therefore differentiating between these processes should be beneficial in any proposed MI therapy.

In similar manner as VEGF, PI3K also plays potentially conflicting roles in the response to I/R injury. The PI3K pathway is generally regarded as antiapoptotic (or procell survival), whereas genetic knockout studies characterize PI3Kγ and -δ as proinflammatory (or antitissue survival). Our findings suggest that this apparent dichotomy can be overcome by tailoring PI3K inhibition to specific isoforms and time periods. PI3K's prosurvival activity has best been demonstrated during the ischemic phase of MI development; because we only inhibited PI3K after reperfusion, disrupting prosurvival signaling in ischemic cardiomyocytes was avoided. Additionally, although total PI3K blockade might be detrimental to tissue survival, the same is not necessarily true for isoform-specific intervention. For example, wortmannin eliminates the cardioprotective effects of numerous agents including insulin (29), IGF1 (30), erythropoietin (31), adrenomedullin (32), and opioids (33), as well as both ischemic pre- and postconditioning (23, 34), demonstrating the potential for at least some PI3K isoforms to ameliorate ischemic tissue damage. Transgenic mice overexpressing a kinase-inactive PI3Kγ in their cardiomyocytes, however, develop equivalent sized infarcts, as do wild-type mice (24), suggesting this isoform at least is not requisite for balancing cardiomyocyte survival. Of course, that these transgenic mice do not show reduced infarcts is not germane to our argument that PI3Kγ/δ inhibition provides cardioprotection, because we propose that systemically administered TG100-115 has as its primary target of action leukocytes and vascular endothelium, not cardiomyocytes.

The antiedema and -inflammatory activities observed upon PI3Kγ/δ inhibition were demonstrated when directed against either receptor tyrosine kinase or GPCR agonists (VEGF or histamine and PAF, respectively), supporting the concept that PI3K inhibition can achieve the broad ligand blocking profile required for effective reduction of reperfusion injury. Two mediators of particular interest were VEGF and PAF. Both are produced by ischemic myocardium (4, 35), and both act directly on EC to promote vascular permeability (36, 37). VEGF-driven edema particularly has been implicated as a major factor underlying infarct progression (26). In addition to inducing edema, PAF also promotes leukocyte adherence to hypoxic endothelium (38), activates neutrophils and platelets (39), and is a negative inotrope (leading to cardiodepression by PI3Kγ signaling) (40). TG100-115's ability to antagonize both VEGF and PAF-

mediated inflammation was therefore a positive step in proposing this compound as a cardioprotectant.

Rodent and porcine MI models confirmed these cardioprotective actions. A major goal was to provide weight to these data by designing studies to aggressive standards. Therefore, although ischemic phases <60 min coupled with <6 h endpoints are commonly used, we adopted 60- to 90-min ischemic periods and measured infarcts 24 h after initiation, as recommended by a National Institutes of Health-convened expert panel (3). Most importantly, all therapeutic interventions were administered after reperfusion rather than during ischemia or even preischemia, as is routinely reported. Adopting these aggressive standards limited the achievable extent of infarct reduction, because considerable myocardial death would have occurred in the time between ischemia onset and therapeutic intervention. Despite this challenge, PI3Kγ/δ inhibition reduced infarct size by $\approx$40% in both rodent- and porcine-based studies. In the rat, TG100-115 achieved maximal efficacy when dosed as late as 3 h after reperfusion (4 h after the initial ischemic injury), and a single dosing on the day of infarction was sufficient to yield a durable functional benefit (improved fractional shortening 4 weeks later). This achievement hopefully serves the goal of producing data better predictive of potential performance in the intended clinical environment, where patients are most likely to receive cardioprotective therapy after diagnosis of an evolving MI if not after reperfusion (3), after meaningful ischemic and even reperfusion injury has already occurred.

In conclusion, we propose that PI3K inhibition represents a promising approach to limiting I/R injuries such as acute MI, provided the appropriate kinase inhibitor can be identified. Consensus is building that isoform specificity must be successfully addressed when developing PI3K inhibitors, with both δ and γ isoforms ranking high as potential targets. For example, an inhibitor slanted toward the γ isoform (but also inhibiting PI3K$\alpha/\beta/\delta$ at $\leq$300 nM) was recently shown to inhibit rheumatoid arthritis and lupus nephritis (41, 42). Our data extend these concepts by demonstrating the value of PI3Kγ/δ inhibition in inflammatory-based but nonautoimmune pathologies. We believe that TG100-115 meets several criteria that support its development as a cardioprotective therapy, in that it is specific against its targets, is deliverable by the clinically appropriate route (i.v.) during the clinically appropriate period (after reperfusion), achieves relatively high efficacy at relatively low doses, and provides maximal efficacy within a relatively wide therapeutic window. Indeed, based on these positive attributes, TG100-115 is currently being studied in acute MI patients when delivered after reperfusion.

Methods

Kinase Inhibitors. TG100-115 [3-[2,4-diamino-6-(3-hydroxyphenyl)pteridin-7-yl]phenol], TG100713 [3-(2,4-diamino-pteridin-6-yl)-phenol], and TG101110 [6-(1H-indol-4-yl)-pteridin-2,4-diamine] were designed by and synthesized at TargeGen; Wortmannin and LY294002 were purchased from Calbiochem (San Diego, CA). Compounds were prepared for *in vitro* assays as DMSO stocks and for *in vivo* assays as either PEG or sulfobutyl ether β-cyclodextrin (CyDex, Lenexa, KS) formulations.

Molecular Modeling. Protein coordinates for human PI3Kγ were taken from RCSB Protein Data Bank entry 1E8Z; additional structures (1E7U, 1E7V, 1E8W, and 1E8Y) were superimposed to examine potential flexibility and binding modes. Compound structures were docked into PI3K active sites using interactive modeling and automated docking software, then minimized in a molecular mechanics program using the consistent force field (CFF) with a distance-dependent dielectric (Insight II and Discover; Accelrys, San Diego, CA). For optimization, all atoms were allowed movement in residues containing at least one atom within 8 Å of any ligand atom. Ribbon models were generated by using YASARA (Yasara Biosciences, Graz, Austria). Complexes were overlaid by using a method that superimposes corresponding carbon α atoms (43), and renderings generated by using Insight II.

Kinase Assays. PI3K reactions were constructed by using recombinant human kinases, 3 μM ATP, phosphatidylinositol substrate, and cofactors, and reaction progression measured by using a luminescent-based detection system to quantify ATP consumption (see *SI Supporting Text*). Protein kinase assays were performed by using commercial screening services (Upstate Biotechnology, Charlottesville, VA; Invitrogen, Carlsbad, CA).

Western Blots. Serum-starved human umbilical vein EC (Cambrex BioScience, Walkersville, MD) were treated for 15 min with test agents (10 μM) or vehicle, followed by a 5-min treatment with 20 ng/ml recombinant human VEGF (PeproTech, Rocky Hill, NJ) or vehicle. Lysates were then processed as Western blots to detect phosphorylated VE-cadherin and ERK1/2 or total ERK2 (see *SI Supporting Text*). For detection of *in vivo* phospho-Akt, BALB/c mice were first dosed i.v. with TG100-115 or vehicle and then injected i.v. at the desired time with 20 ng of VEGF or saline. Lungs were explanted after 5 min and processed to lysates, and Western blots performed as described.

Cell Proliferation Assays. Human umbilical vein EC plated in 96-well cluster plates (5,000 cells/well) were cultured in assay medium (containing 0.5% serum and 50 ng/ml VEGF) in the presence or absence of test compounds (10 μM), and cell numbers were quantified by XTT assay (Promega, Madison, WI) 24, 48, or 72 h later.

Miles Assay. All animal studies followed current NIH Guidelines for the Use of Laboratory Animals and were performed according to Institutional Animal Care and Use Committee-approved protocols. Sprague–Dawley rats (175–200 g) were dosed i.v. with either TG100-115 (1 mg/kg) or vehicle, and 1–4 h later Evans blue dye (Sigma, St. Louis, MO) was administered i.v. as 500 μl of a 2% sterile saline solution. Immediately after dye injection, animals were injected intradermally on each shaved flank with 100 μl of saline, VEGF (2 μg/ml stock), or histamine (10 μg/ml stock). Thirty minutes later, injection sites were photographed.

Hindpaw Inflammation. Sprague–Dawley rats (275–300 g) were dosed i.v. with either TG100-115 (5 mg/kg) or vehicle and then injected 30 min later in the plantar hindlimb surface with 100 μl of dextran suspension (Sephadex G-75 suspended at 80 mg/ml in saline and autoclaved) or PAF (16 pM c-PAF stock; Biomol International, Plymouth Meeting, PA). Animals were administered buprenorphine (0.01 mg/kg, s.c.) to control pain, and 3 h later paw dimensions were measured to the nearest 0.1 mm using calipers. Volume was then calculated and expressed as mm^3; injection sites were harvested and processed to H&E-stained paraffin sections.

Animal MI Models. Rodent and porcine MI models are fully described in *SI Supporting Text.* Briefly, Sprague–Dawley rats were subjected to 60 min of complete left anterior descending coronary artery (LAD) occlusion followed by complete reperfusion; TG100-115 or vehicle was delivered i.v. at 0–3 h after reperfusion. Twenty-four hours later, LAD occlusion was repeated, animals were injected with Evans blue dye to delineate perfused from ischemic areas, and then heart sections were stained in triphenyltetrazolium chloride to delineate viable tissue from infarct and photographs were processed using an image analysis software program to quantify infarct area. Alternatively, LV function was assessed using echocardiography at 4 weeks by determining percent fractional shortening from long

axis images (by personnel blinded as to treatment identity). For the porcine model, farm swine were subjected to 90 min of complete LAD occlusion followed by complete reperfusion; TG100-115 or vehicle was delivered i.v. 30 min after reperfusion, and infarct area was determined as in the rodent model at 24 h.

Statistics. Two group comparisons were made using unpaired Student's *t* tests, and multiple group analyses using one-way ANOVA with post hoc Dunnett's tests (SigmaStat software; SPSS, Chicago, IL). If Dunnett's tests showed statistical differences for more than one group compared with controls, a second ANOVA for intergroup differences was performed using the Student–Newman–Keuls method as the post hoc test. Statistical significance was defined as $P < 0.05$.

We are thankful for the excellent technical support of Cyrus Virata, Jann Key, Silva Stoughton, Chris Jacob, Ehab Hanna, Hong Zhu, Dan Lohse, Chi Ching Mak (TargeGen, Inc.), Jason Kang (BioPredict), Oi Ling Kwan, Feliz Garcia Bannach (University of California at San Diego), Mark Cunningham, and the staff of Charles River Laboratories (Southbridge, MA), and Mark Johnson and the staff of MPI Research (Mattawan, MI). D.C. is supported by Grants HL57900 and HL78912 from the National Institutes of Health.

1. Crow MT, Mani K, Nam YJ, Kitsis RN (2004) *Circ Res* 95:957–970.
2. Frangogiannis NG, Smith CW, Entman ML (2002) *Cardiovasc Res* 53:31–47.
3. Bolli R, Becker L, Gross G, Mentzer R, Jr, Balshaw D, Lathrop DA (2004) *Circ Res* 95:125–134.
4. Lee SH, Wolf PL, Escudero R, Deutsch R, Jamieson SW, Thistlethwaite PA (2000) *N Engl J Med* 342:626–633.
5. Montrucchio G, Alloatti G, Camussi G (2000) *Physiol Rev* 80:1669–1699.
6. Herskowitz A, Choi S, Ansari AA, Wesselingh S (1995) *Am J Pathol* 146:419–428.
7. Coker SJ, Parratt JR, Ledingham IM, Zeitlin IJ (1981) *Nature* 291:323–324.
8. Lee CC, Appleyard RF, Byrne JG, Cohn LH (1993) *Cardiovasc Res* 27:770–773.
9. Masini E, Bianchi S, Gambassi F, Palmerani B, Pistelli A, Carlomagno L, Mannaioni PF (1990) *Agents Actions* 30:198–201.
10. Erlich JH, Boyle EM, Labriola J, Kovacich JC, Santucci RA, Fearns C, Morgan EN, Yun W, Luther T, Kojikawa, O. *et al.* (2000) *Am J Pathol* 157:1849–1862.
11. Engler RL, Roth DM, del Balzo U, Ito BR (1991) *FASEB J* 5:2983–2991.
12. Laffargue M, Calvez R, Finan P, Trifilieff A, Barbier M, Altruda F, Hirsch E, Wymann MP (2002) *Immunity* 16:441–451.
13. Hirsch E, Katanaev VL, Garlanda C, Azzolino O, Pirola L, Silengo L, Sozzani S, Mantovani A, Altruda F, Wymann MP (2000) *Science* 287:1049–1053.
14. Hirsch E, Bosco O, Tropel P, Laffargue M, Calvez R, Altruda F, Wymann M, Montrucchio G (2001) *FASEB J* 15:2019–2021.
15. Yum HK, Arcaroli J, Kupfner J, Shenkar R, Penninger JM, Sasaki T, Yang KY, Park JS, Abraham E (2001) *J Immunol* 167:6601–6608.
16. Hannigan M, Zhan L, Li Z, Ai Y, Wu D, Huang CK (2002) *Proc Natl Acad Sci USA* 99:3603–3608.
17. Ali K, Bilancio A, Thomas M, Pearce W, Gilfillan AM, Tkaczyk C, Kuehn N, Gray A, Giddings J, Peskett E, *et al.* (2004) *Nature* 431:1007–1011.
18. Vanhaesebroeck B, Ali K, Bilancio A, Geering B, Foukas LC (2005) *Trends Biochem Sci* 30:194–204.
19. Amaravadi R, Thompson CB (2005) *J Clin Invest* 115:2618–2624.
20. Hausenloy DJ, Yellon DM (2004) *Cardiovasc Res* 61:448–460.
21. Nagoshi T, Matsui T, Aoyama T, Leri A, Anversa P, Li L, Ogawa W, del Monte F, Gwathmey JK, Grazette L, *et al.* (2005) *J Clin Invest* 115:2128–2138.
22. Young LH, Ikeda Y, Scalia R, Lefer AM (2000) *J Pharmacol Exp Ther* 295:37–43.
23. Tsang A, Hausenloy DJ, Mocanu MM, Yellon DM (2004) *Circ Res* 95:230–232.
24. Tong H, Rockman HA, Koch WJ, Steenbergen C, Murphy E (2004) *Circ Res* 94:1133–1141.
25. Meadows KN, Bryant P, Pumiglia K (2001) *J Biol Chem* 276:49289–49298.
26. Weis S, Shintani S, Weber A, Kirchmair R, Wood M, Cravens A, McSharry H, Iwakura A, Yoon YS, Himes N, *et al.* (2004) *J Clin Invest* 113:885–894.
27. Klingenberg HG, Dorner H (1975) *Exp Pathol* 10:333–337.
28. Jiang BH, Zheng JZ, Aoki M, Vogt PK (2000) *Proc Natl Acad Sci USA* 97:1749–1753.
29. Jonassen AK, Sack MN, Mjos OD, Yellon DM (2001) *Circ Res* 89:1191–1198.
30. Fujio Y, Nguyen T, Wencker D, Kitsis RN, Walsh K (2000) *Circulation* 101:660–667.
31. Cai Z, Semenza GL (2004) *Circulation* 109:2050–2053.
32. Okumura H, Nagaya N, Itoh T, Okano I, Hino J, Mori K, Tsukamoto Y, Ishibashi-Ueda H, Miwa S, Tambara K, *et al.* (2004) *Circulation* 109:242–248.
33. Gross ER, Hsu AK, Gross GJ (2004) *Circ Res* 94:960–966.
34. Tong H, Chen W, Steenbergen C, Murphy E (2000) *Circ Res* 87:309–315.
35. Berti F, Magni F, Rossoni G, De Angelis L, Galli G (1990) *J Cardiovasc Pharmacol* 16:727–732.
36. Olander JV, Connolly DT, DeLarco JE (1991) *Biochem Biophys Res Commun* 175:68–76.
37. Bussolino F, Camussi G, Aglietta M, Braquet P, Bosia A, Pescarmona G, Sanavio F, D'Urso N, Marchisio PC (1987) *J Immunol* 139:2439–2446.
38. Milhoan KA, Lane TA, Bloor CM (1992) *Am J Physiol* 263:H956–H962.
39. Prescott SM, Zimmerman GA, Stafforini DM, McIntyre TM (2000) *Annu Rev Biochem* 69:419–445, 419–445.
40. Alloatti G, Levi R, Malan D, Del Sorbo L, Bosco O, Barberis L, Marcantoni A, Bedendi I, Penna C, Azzolino O, *et al.* (2003) *Cardiovasc Res* 60:242–249.
41. Camps M, Ruckle T, Ji H, Ardissone V, Rintelen F, Shaw J, Ferrandi C, Chabert C, Gillieron C, Francon B, *et al.* (2005) *Nat Med* 11:936–943.
42. Barber DF, Bartolome A, Hernandez C, Flores JM, Redondo C, Fernandez-Arias C, Camps M, Ruckle T, Schwarz MK, Rodriguez S, *et al.* (2005) *Nat Med* 11:933–935.
43. Lesk AM (1997) *Fold Des* 2:S12–S14.